


Geomagnetically Induced Currents: Principles

Denny M. Oliveira^{1,2}  · Chigomezio M. Ngwira^{1,3}

Received: 14 June 2017 / Published online: 15 August 2017
© Sociedade Brasileira de Física 2017

Abstract The geospace, or the space environment near Earth, is constantly subjected to changes in the solar wind flow generated at the Sun. The study of this environment variability is called Space Weather. Examples of effects resulting from this variability are the occurrence of powerful solar disturbances, such as coronal mass ejections (CMEs). The impact of CMEs on the Earth's magnetosphere very often greatly perturbs the geomagnetic field causing the occurrence of geomagnetic storms. Such extremely variable geomagnetic fields trigger geomagnetic effects measurable not only in the geospace but also in the ionosphere, upper atmosphere, and on and in the ground. For example, during extreme cases, rapidly changing geomagnetic fields generate intense geomagnetically induced currents (GICs). Intense GICs can cause dramatic effects on man-made technological systems, such as damage to high-voltage power transmission transformers leading to interruption of power supply, and/or corrosion of oil and gas pipelines. These space weather effects can in turn lead to severe economic losses. In this paper, we supply the reader with theoretical concepts related to GICs as well as their general consequences. As an example, we discuss the GIC effects on a North American power grid located in mid-latitude regions during the 13–14 March 1989 extreme geomagnetic storm.

That was the most extreme storm that occurred in the space era age.

Keywords Solar-terrestrial connections · Geospace environment · Geomagnetic storms · Geomagnetically induced currents

1 Introduction

The space environment in the Earth's vicinity, or the geospace, is directly affected by the flow of charged particles generated at the Sun, named the solar wind plasma [27]. Solar wind particles and the embedded magnetic field, commonly called interplanetary magnetic field or IMF, interact directly with the Earth's magnetic field, and carves out a region in space called the magnetosphere (see Fig. 1). The speed and flow direction of the solar wind along with the IMF orientation controls the shape and size of the magnetosphere [56]. When such solar disturbances encounter the terrestrial magnetosphere, a myriad of effects may arise both in the geospace and on the ground [27, 29]. Studies of these interactions and their subsequent effects are subject of a discipline named Space Weather [12, 27].

The IMF is attached to the solar wind due to frozen-in conditions [57]. If the north-south component of the IMF is directed downwards, i.e., $B_z < 0$, more solar wind energy and momentum are allowed to enter the magnetosphere [10]. This process is called magnetic reconnection [18]. As a result, energized plasma coming from the magnetosphere may generate geomagnetic effects detectable in the geospace [67], upper atmosphere [48, 60], ionosphere [39, 43, 45, 60], and on the ground [20, 25, 40].

The most geoeffective solar disturbances are named coronal mass ejections (CMEs) [19, 59]. When CMEs strike

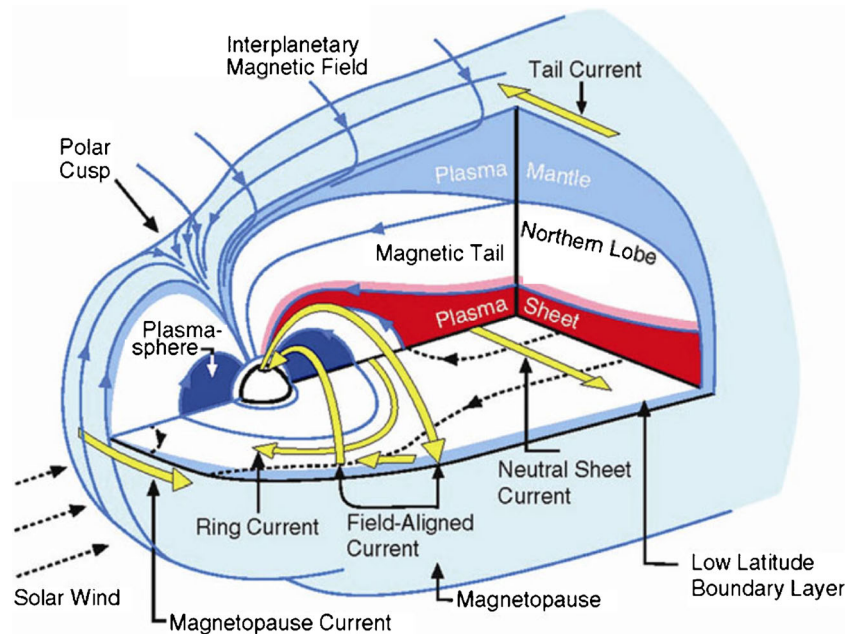
✉ Denny M. Oliveira
denny.m.deoliveira@nasa.gov

¹ NASA Goddard Space Flight Center, Greenbelt, MD, USA

² Goddard Planetary Heliophysics Institute, University of Maryland Baltimore County, Baltimore, MD, USA

³ Department of Physics, Catholic University of America, Washington, DC, USA

Fig. 1 The Earth's magnetosphere and its current system. Figure downloaded from http://www.mssl.ucl.ac.uk/www_plasma/main.php



Earth, the first most dramatic effect that takes place almost instantaneously is the storm sudden commencement (SSC), which is the signature of a sharp geomagnetic field increase resulting from the sudden magnetosphere compression. This phenomenon is usually associated with shock waves driven by the CME leading edge or CME shock/sheath region [3, 33–35, 44, 46, 47]. CMEs carry magnetic structures with them, frequently named magnetic clouds. Magnetic clouds have intense magnetic fields whose north-south component rotates at high rates while CMEs travel in the interplanetary space [19, 59]. The B_z component then interacts with the north-ward dayside geomagnetic field causing magnetic reconnection to occur [61]. As a result, magnetic reconnection occurs whose intensity will closely depend upon how negative B_z is and how long it is sustained throughout the storm period [16, 17].

Modern technological infrastructures, such as power grids, oil and gas pipelines, and communication systems, are often affected by severe solar disturbances. For example, the impact of CMEs as described above on the Earth's magnetosphere can generate geomagnetically induced currents (GICs). GICs result from highly variable currents in the magnetosphere-ionosphere system that induce an electric field on the Earth's surface [5, 25, 37, 50, 51]. The effects of GICs are notable not only in high-latitude regions [42, 54, 65, 66], but also in mid-low latitudes and equatorial regions [1, 8, 9, 38, 40, 68, 69]. Although GICs can be highly intensified during severe storm times, the impact of shocks followed by compressions have been of interest since a growing number of electric power infrastructures are located in several regions at different latitudes, including equatorial regions [4, 8, 14, 68]. Such effects have led

policy makers to initiate measures to assess risks and protect human-made assets not only on the ground, but in space as well (see, e.g., [22], and references therein).

The main goal of this paper is to provide the basic theory and observational concepts associated with GICs, supported with several references to guide the reader. In Section 2, we discuss the nature and nomenclature frequently used in regarding geomagnetic storms, focusing on extreme events. Section 3 shows the most important theoretical concepts used to calculate GICs with a summary of the most important GIC equations. As an example of an extreme and rare event, we choose the 13–14 March 1989 geomagnetic storm to illustrate its effects on the GIC production in the ground. Section 4 discusses the storm and GIC effects. Finally, Section 5 summarizes and concludes the paper.

2 Nature and Classification of Geomagnetic Storms

As previously discussed in the introductory section above, CME-driven geomagnetic storms are characterized by the interaction of two distinct regions with the Earth's magnetosphere. First, the CME leading edge whose impact causes the horizontal field component to increase, or an SSC. This is the initial phase of the storm. When the magnetic structure arrives at Earth, due to magnetic reconnection, this horizontal field component is highly depressed in a time frame of one to a few hours, or even a few days, until its recovery [28]. This characterizes the storm main phase and storm recovery phase. The depression in the horizontal magnetic field measured at the ground is caused by an intensification of the ring current (10–3000 keV electrons and ions coming

from the magnetosphere) that flow around the Earth in the dusk-dawn direction.

Geomagnetic storm intensities are measured by a very popular index called disturbance storm index, or Dst. The Dst index has a time resolution of one hour and is compiled from measurements obtained by ground magnetometers at stations located in middle latitudes. Although Dst is still commonly used today, another index which seems to be preferred to capture shorter time scale magnetosphere dynamics is the symmetric ring current index, or SYM-H. This index is similar to the Dst index, but with a finer time resolution of one minute, as first suggested by Iyemori [21]. Both Dst and SYM-H index data can be downloaded from the website of the World Data Center located in Kyoto, Japan (<http://wdc.kugi.kyoto-u.ac.jp/index.html>). In this paper, we will use the term Dst as a general term to describe geomagnetic activity. The SYM-H term will be used when referring specifically to the one-minute time resolution index.

Geomagnetic storms are frequently classified according to their intensity as quantified by the minimum value of the Dst index occurring at the end of the storm main phase. There are several different ways to classify storms. These storm classifications may differ among the space science community depending on the study. For example, what one would consider a moderate storm, another one would consider an intense storm, and so on. Perhaps the most used nomenclature was suggested by Gonzalez et al. [16] and will be used here. A weak storm usually has a minimum Dst of -30 nT; in the case of a moderate storm, -50 nT $<$ Dst $<$ -30 nT; and intense storms, -100 nT $<$ Dst $<$ -50 nT. Storms with these intensities occur very often throughout a solar cycle. Superintense geomagnetic storms (-500 $<$ Dst $<$ -100 nT) are relatively rare. Here the term extreme event is reserved for storms with Dst $<$ -500 nT. For example, only one extreme storm occurred during the space age era, namely the storm of 13–14 March 1989 [2]. The most intense extreme event that exists on record is the Carrington event which occurred in the period 1–2 September 1859. According to modern estimates [62], that storm had an SSC with amplitude of ~ 120 nT with an unprecedented maximum H-component depression magnitude of ~ 1600 nT at a low latitude station. The main phase of that extraordinary storm lasted for ~ 1.5 h, which is typical for extreme events [28]. General properties of extreme events estimated by historical data can be found in the literature [28, 62, 63]. Table 1 summarizes the storm nomenclature used in this paper, along with their correspondent minimum B_z components.

In spite of being rare, the occurrence of extreme storms could be catastrophic to modern day technology. It is widely considered that a Carrington-like storm could cause severe damage to human assets not only in space, but also on the ground, as discussed in the literature [28, 31, 41, 62].

Table 1 Nomenclature often used in classifications of geomagnetic storms

Storm	Minimum	Minimum	Time
Classification	Dst (nT)	B_z (nT)	Duration
Weak	-30	-3	1 h
Moderate	-50	-5	2 h
Intense	-100	-10	3 h
Superintense	-500	-50	> 3 h
Extreme	< -500	< -50	< 3 h

However, a recent study has shown that such an event or even a stronger event might occur with probability 3–10% in the next 100 years or so [55].

3 Generation and Computation of GICs

Basically, GICs on the ground occur at the end of a complex space weather chain of events triggered by solar eruptions. The dynamic interaction between the disturbed solar wind and the Earth's magnetosphere causes intense variation of near-space electric current systems that produce rapid changes in the surface geomagnetic field.

Fundamentally, the physical concept of the flow of GICs is associated with Faraday's law of induction, i.e., changing magnetic fields induce electric currents in conductors. This law can be expressed mathematically as

$$\nabla \times \mathbf{E} = - \frac{\partial \mathbf{B}}{\partial t} \quad (1)$$

thereby relating the temporal variation of the geomagnetic field to the formation of the geoelectric field. The induced geoelectric field inside the Earth then drives GICs in ground systems according to Ohm's law $\mathbf{J} = \sigma \mathbf{E}$. This induced geoelectric field is independent of the technological system but primarily depends on the magnetosphere and ionosphere currents along with secondary effects introduced by the Earth's geology [49].

Computation of GIC flowing through a particular network node involves a two-step approach [50, 51]. The first step is of geophysical nature requiring the estimation of the geoelectric field based on the knowledge of the magnetosphere-ionosphere currents and ground conductivity structure. The second step is the engineering part in which the currents flowing in the system are estimated based on the determined geoelectric field and detailed information about the particular ground system.

Since the geoelectric field controls the currents that flow on ground-based systems, it is therefore the primary quantity that determines the magnitude of GICs. The simplest

geolectric field model assumes that a plane wave is propagated vertically downwards and that the Earth is a uniform (or a layered) half-space with conductivity σ [7].

If we adopt a single frequency ω and a reference frame in which the X and Y axes lie in the horizontal plane, the horizontal geolectric field components can be given in terms of the perpendicular horizontal geomagnetic field component $B_{y,x}$ as

$$E_{x,y} = \pm \sqrt{\frac{\omega}{\mu_0 \sigma}} e^{\frac{i\pi}{4}} B_{y,x} \quad (2)$$

where μ_0 is the permeability of free space. To eliminate significant attenuation of external electromagnetic fields, the layer of air between the ground and the ionosphere is assumed to have zero conductivity.

Equation (2) is the “basic equation of magnetotellurics” that stipulates the basis for deriving the Earth’s conductivity using electric (or telluric) and magnetic measurements recorded at the surface. The plane wave method is a well-established and commonly used method in GIC applications [4, 38, 40, 51, 54, 66].

Once the E-field is known, it is relatively straightforward to carry out the engineering step for any ground system (e.g., [37, 50]). Treating the geolectric field as spatially constant and if the network coefficients are known, then the GIC can be calculated according to the equation

$$\text{GIC}(t) = a E_x(t) + b E_y(t) \quad (3)$$

where a and b are the network-specific coefficients at each network node depending only on the resistance and geometrical composition of a system [65]. Equation (3), widely referred to as the “GIC equation,” is a purely engineering task requiring an accurate description of the system parameters. For further details regarding this step, interested readers are encouraged to consult Lehtinen and Pirjola [30] and/or Viljanen and Pitjola [65], and references therein.

4 The 13–14 March 1989 Extreme Event

4.1 Storm SYM-H Profile

The 13–14 March 1989 geomagnetic storm is the only storm event that took place in the space age era that agrees with our definition of extreme storms, as expressed by Table 1. Unfortunately, for this storm, there are neither solar wind nor IMF data available because there were no spacecraft upstream of the Earth to measure the solar wind and IMF properties. The only data available for that storm come from measurements obtained by ground magnetometers.

Figure 2 shows the SYM-H profile of the 13–14 March 1989 geomagnetic storm. The time range of that plot goes from 0000 UT of 12 March 1989 to 0000 UT of 15 March

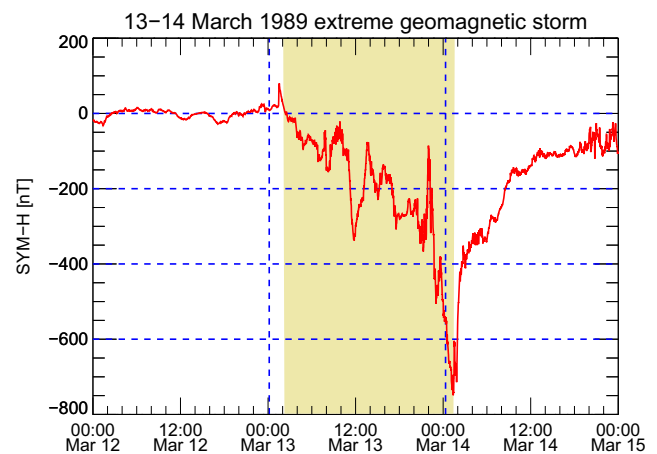


Fig. 2 Three-day range of SYM-H data, in nT, for the 13–14 March 1989 geomagnetic storm. The highlighted region corresponds to the complex developing of the storm main phase which occurred mostly on the 13th of March. The non-highlighted regions corresponds to the quiet time (mostly during the 12th of March), and the recovery phase, (mostly during the 14th of March). The abrupt change in SYM-H seen a few minutes after 0200 UT (day 13) marks the onset of the storm initial phase, or the occurrence of an SSC event

1989. Needless to say, this storm presented a very interesting and complex behavior. The storm can be divided in the following phases: the quiet time, mostly on the 12th of March; the storm main phase, mostly on the 13th of March, highlighted in the figure; and storm recovery phase, mostly on the 14th of March. The minimum Dst value was ~ -589 nT, and the minimum SYM-H value was ~ -710 nT, which occurred approximately at 0100 UT on 14 March 1989 corresponding to the end of a long and complex main phase with duration of almost 24 hours. From the GIC standpoint, it is important to note that the intensity of GICs is closely related to the rate of change of the geomagnetic field, as expressed in (1), rather than the peak value of the Dst index.

The storm initial phase occurred at ~ 0200 UT on the 13th of March, starting with an abrupt increase in the SYM-H index before reaching an amplitude of about 40 nT, probably due to the impact of a high-speed CME. Among other minor SSC events, another major one took place, with magnitude ~ 80 nT, presumably due to the impact of another fast CME. The sequence of several CME impacts causes the SYM-H index to decrease throughout the 13th of March. For example, several deep negative excursions can be identified during that day: ~ 0230 – 0900 UT (minimum SYM-H of -150 nT; ~ 1100 – 1200 UT, minimum SYM-H -260 nT; a complex multi-main phase period occurs between ~ 1800 – 2200 UT with several decreases of the SYM-H index which are most likely related to CMEs with strongly negative B_z components. Approximately at the end of the storm main phase, SYM-H decreases sharply in the period of ~ 2300 UT of the 13th of March to the ~ 0100 UT of the 14th of March with an amplitude as strong as 350

nT, when SYM-H reached its minimum value. After ~ 0100 UT of 14 March 1989, the magnetosphere starts gradually to recover and it takes over a day to return to its steady state. As a result, the overall and complex main phase of the storm was a result of the combination of several main phases presumably generated by a sequence of the impacts of several high-speed CMEs on the Earth's magnetosphere.

Based on the theoretical framework presented in the previous section, it is clear that the extreme storm of 13–14 March 1989 caused extreme effects on the ground due to the induction of GICs. In the next section, we will discuss those effects.

4.2 GIC Effects

The March 1989 storm is definitely the largest geomagnetic storm of the space age. The resulting GICs caused widespread space weather effects. It is reported that in North America, these effects appeared at six different times during the entire storm period [6, and references therein]. The most serious impact of the storm occurred at 0245 EST on March 13 when large amplitude GICs caused failure of Hydro-Quebec power network grid. The power outage was a result of broad transformer saturation producing harmonics that in turn caused tripping of several static VAR compensators (e.g., [5, 6], and references therein). For an in-depth discussion on the impact of GICs on electric power utilities, readers are encouraged to consult Molinski [36].

Usually GIC effects are investigated for individual ground stations around the globe. Ground magnetometer data of individual stations can be found, with time resolution of 1 minute, at the SuperMAG collaboration website (<http://supermag.jhuapl.edu> and supermag.uib.no) and the United States Geological Survey (USGS) website (<https://geomag.usgs.gov/products/downloads.php>).

Although the prompt and most dramatic GIC effects occur in power transmission systems located in high latitude regions, it is important to note that this extreme storm did in fact also affect power transmission systems in mid-latitudes. As reported by Carter et al. [8], GIC enhancements in mid- and low-latitude regions are also important due to high increase in the number of power transmission lines in those regions located mainly in developing countries.

Shown in Fig. 3 is a response of the recorded horizontal geomagnetic field B_x and B_y components and the rate-of-change $d\mathbf{H}/dt$ for Fredericksburg station (Latitude 38.20° N, Longitude 77.32° W) in USA for the 13 Mar 1989 extreme storm. This figure covers the main phase and recovery phase of the storm. During the development of the storm main phase, some variations in B_x and B_y are seen presumably resulting from multiple impacts of CMEs on the 13 Mar 1989, as seen in Fig. 2 for the SYM-H response. The horizontal magnetic field variation presents a few peaks

ranging from 50 nT to approximately 330 nT during the 13th of March, well timed with enhancements in B_x and B_y , in random time intervals of 2–6 hours. In addition, at approximately 2000 UT of the 13th of March, B_x is strongly enhanced, and a B_y enhancement follows within near 1 hour. The corresponding $d\mathbf{H}/dt$ data also contain intense variations during this interval, which are quite extreme for this typical mid-latitude station. However, this scenario is not surprising during extreme storms like 13–14 March 1989 when auroral current, which is one of the major drivers of GICs, can expand to lower latitudes (see e.g., [11, 24, 40, 41]).

One of the main GIC effects on ground-based equipment occurs on power grid transformers. During times of intense GICs, transformers can be seriously damaged and even completely destructed by intense heat caused by the flow of GICs. As widely reported in the literature, the shape and size of transformers control the local heat and subsequent increase in temperature in vital functional areas of transformers (see, e.g., [13, 23, 52]).

An example of direct effects caused by GICs induced at a mid-latitude power grid station is shown in Fig. 4, extracted from Kappenman [23]. This figure shows internal heat effects on a transformer located at the Salem Nuclear Plant in Lower Alloways Creek, N.J. That was a large transformer connected to the 500 kV grid transmission of the Salem station. The image on left shows the transformer under natural conditions. The two images on right show a picture of some of the transformer's components after the 13–14 March 1989 extreme geomagnetic storm. The intense GICs caused a severe melting down of the transformer paper tape winding insulation themselves, even though they were immersed in oil for cooling and insulation (for more technical details, see [23]). Therefore, intense GIC enhancements can destroy power grid equipment and lead so severe economic losses. For more details on the assessment of GIC impacts on power grid distributions and the subsequent economic consequences in recent years, see Schrijver et al. [58].

Finally, we would like to mention another period of intense geomagnetic activity caused by the impact of fast CMEs on Earth, namely the Halloween storms [32]. These storms occurred on the period of 29–31 October 2003, with minimum Dst around -400 nT [64]. As reported by Kappenman [26], in spite of their classification as super intense storms, the Halloween events caused modest variations in the horizontal magnetic field, leading to unexpectedly low GIC intensifications, at least in the North American sector. Indeed, these storms caused blackout in Sweden [53] and severe damage to power grids in South Africa [15]. Kappenman [26] attributed such modest GIC variations to the use of similar geomagnetic indices to compare geomagnetic effects in different regions. As a result, the prediction

Fig. 3 Geomagnetic field response during the 13–14 March 1989 super storm at Fredericksburg, USA. *Top* and *middle panel* display the horizontal geomagnetic field B_x and B_y component, respectively. The *bottom panel* shows the rate of change of H-component. The data are sample at 1-minute resolution

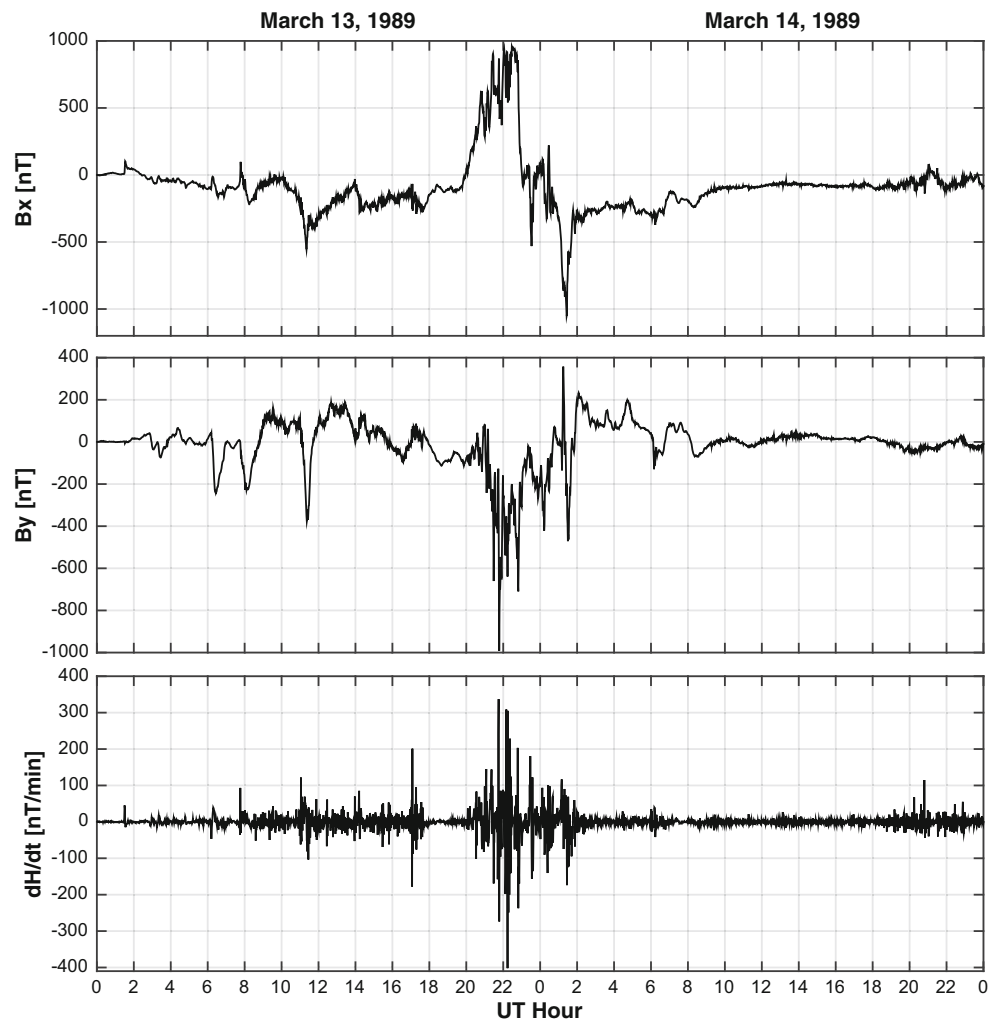


Fig. 4 Transformer damaged by an intense internal heating caused by the superintense 13–14 March 1989 geomagnetic storm. *Left image*: transformer under normal conditions. *Two right images*: details of the components whose melting down was caused due to severe GIC increases. Figure taken from Kappenman [23]

of GIC effects based on such analysis would lead to overestimated GIC intensifications and subsequent power grid consequences. A detailed comparison between the GIC effects of the Halloween storms and the 13–14 March 1989 extreme event is performed by Kappenman [26].

5 Summary and Conclusion

In this paper, we reviewed some basic ideas of the effects resulting from solar-terrestrial connections, with emphasis on geomagnetic storms. We presented some equations to illustrate the theoretical basis of GIC calculations. Our main focus was on the basic principles of GIC generation on the ground and their threats and consequences to modern technology.

As an example for discussion, we chose the extreme geomagnetic storm of 13–14 March 1989. That storm was the largest storm in the space era, with minimum SYM-H

index of approximately -710 nT at the end of its complex and intricate 23-h main phase. Although there are no solar wind/IMF data available for that particular storm, due to its SYM-H profile, it is speculated that storm event was caused by the impact of successive fast CMEs on the magnetosphere. The storm took over a day to recover from that extreme event.

The ground effects caused by that extreme geomagnetic storm were analyzed in some details to a particular mid-latitude location. The horizontal geomagnetic field component, B_x , showed a gradual increase at 2000 UT of 13 March, and the B_y component showed a sharper increase around the same time as well. Due to this high variability, intense GICs were created within approximately 2 h. As a result, as illustrated by Fig. 4, the transformer of the Salem Nuclear Plant in Lower Alloways Creek, N.J. undertook severe damage. The transformer's paper tape winding and the winding themselves melted down due to an extremely high GIC peak that was associated with a geomagnetic rate-of-change magnitude of ~ 400 nT/min, even though the whole system was immersed in oil used for cooling and isolation.

Finally, we emphasize the importance of the study of Space Weather not only as an academic discipline, but also as a branch of science with great importance in assessing the protection to assure integrity and long useful life of human assets in space and on the ground.

Acknowledgements Dr. Denny Oliveira acknowledges NASA for the financial support provided by grant NNH13ZDA001N-HSR to UMBC/GPHI. Dr. Chigomezio Ngwira was supported by NASA Grant NNG11PL10A 670.157 to CUA/IACS. The authors very kindly thank an anonymous reviewer for carefully evaluating this manuscript.

References

- B.O. Adebesein, A. Pulkkinen, C.M. Ngwira, The interplanetary and magnetospheric causes of extreme dB/dt at equatorial locations. *Geophys. Res. Lett.* **43**(22), 11,501–11,509 (2016). <https://doi.org/10.1002/2016GL071526>
- J. Allen, H. Sauer, L. Frank, P. Reiff, Effects of the March 1989 solar activity. *Eos Trans. AGU* **70**(46), 1479–1488 (1989). <https://doi.org/10.1029/89EO00409>
- T. Araki, A. Shinbori, Relationship between solar wind dynamic pressure and amplitude of geomagnetic sudden commencement (SC). *Earth Planets Space* **68**(9), 1–7 (2016). <https://doi.org/10.1186/s40623-016-0444-y>
- C.S. Barbosa, G.A. Hartmann, K.J. Pinheiro, Numerical modeling of geomagnetically induced currents in a Brazilian transmission line. *Adv. Space Res.* **55**(4) (2015). <https://doi.org/10.1016/j.asr.2014.11.008>
- L. Bolduc, GIC observations and studies in the hydro-Québec power system. *J. Atmos. Sol. Terr. Phys.* **64**(16), 1793–1802 (2002). [https://doi.org/10.1016/S1364-6826\(02\)00128-1](https://doi.org/10.1016/S1364-6826(02)00128-1)
- D.H. Boteler, In *Space Weather, Geophysical Monograph Series*, ed. by P. Song, H.J. Singer, G.L. Siscoe. Space weather effects on power systems, Vol. 125 (American Geophysical Union, Washington, DC, 2001), pp. 347–352. <https://doi.org/10.1029/GM125p0347>
- L. Cagniard, Basic theory of the magneto-telluric method of geophysical prospecting. *Geophysics* **18**(3), 605–635 (1953). <https://doi.org/10.1190/1.1437915>
- B.A. Carter, E. Yizengaw, R. Pradipta, A.J. Halford, R. Norman, K. Zhang, Interplanetary shocks and the resulting geomagnetically induced currents at the equator. *Geophys. Res. Lett.* **42**(16), 6554–6559 (2015). <https://doi.org/10.1002/2015GL065060>
- B.A. Carter, E. Yizengaw, R. Pradipta, J.M. Weygand, M. Piersanti, A. Pulkkinen, M.B. Moldwin, R. Norman, K. Zhang, Geomagnetically induced currents around the world during the March 17, 2015 storm. *J. Geophys. Res. Space Phys.* (2016). <https://doi.org/10.1002/2016JA023344>
- J.W. Dungey, Interplanetary magnetic field and the auroral zones. *Phys. Rev. Lett.* **6**(2), 47–48 (1961). <http://doi.org/10.1103/PhysRevLett.6.47>
- Y. Ebihara, M.-C. Fok, S. Sazykin, M.F. Thomsen, M.R. Hairston, D.S. Evans, F.J. Rich, M. Ejiri, Ring current and the magnetosphere-ionosphere coupling during the superstorm of 20 November 2003. *J. Geophys. Res.* **110**(A9) (2005). <https://doi.org/10.1029/2004JA010924>
- E. Echer, W.D. Gonzalez, F.L. Guarnieri, A.D. Lago, L.E.A. Vieira, Introduction to space weather. *Adv. Space Res.* **35**(5), 855–865 (2005). <https://doi.org/10.1016/j.asr.2005.02.098>
- I.A. Erinmez, J.G. Kappenman, W.A. Radasky, Management of the geomagnetically induced current risks on the national grid company's electric power transmission system. *J. Atmos. Sol. Terr. Phys.* **63**(5–6), 743–756 (2002). [https://doi.org/10.1016/S1364-6826\(02\)00036-6](https://doi.org/10.1016/S1364-6826(02)00036-6)
- R.A.D. Fiori, D.H. Boteler, D.M. Gillies, Assessment of gic risk due to geomagnetic sudden commencements and identification of the current systems responsible. *Space Weather* **12**(1), 76–91 (2014). <https://doi.org/10.1002/2013SW000967>
- C. Gaunt, G. Coetzee, in *Power Tech, 2007 IEEE Lausanne*. Transformer Failures in Regions Incorrectly Considered to have Low GIC-Risk (Switzerland, Lausanne, 2007) pp. 807–812. <https://doi.org/10.1109/PCT.2007.4538419>
- W.D. Gonzalez, J.A. Joselyn, Y. Kamide, H.W. Kroehl, G. Rostoker, B.T. Tsurutani, V.M. Vasyliūnas, What is a geomagnetic storm. *J. Geophys. Res.* **99**(A4), 5771–5792 (1994). <https://doi.org/10.1029/93JA02867>
- W.D. Gonzalez, B.T. Tsurutani, A.L. Clúa de Gonzalez, Interplanetary origin of geomagnetic storms. *Space Sci. Rev.* **88**(3–4), 529–562 (1999). <https://doi.org/10.1023/A:1005160129098>
- W.D. Gonzalez, E.N. Parker, F.S. Mozer, V.M. Vasyliūnas, P.L. Pritchett, H. Karimabadi, P.A. Cassak, J.D. Scudder, M. Yamada, R.M. Kulsrud, D.K. Less, in *Magnetic Reconnection*, ed. by W.D. Gonzalez, E.N. Parker. Fundamental Concepts Associated with Magnetic Reconnection, Vol. 427 (Springer International Publishing, Cham, Switzerland, 2016), pp. 132. https://doi.org/10.1007/978-3-319-26432-5_1
- J.T. Gosling, In *Coronal Mass Ejections, Geophysical Monograph Series*, ed. by N. Crooker, J.A. Joselyn, J. Feynman. Coronal mass ejections: an overview, Vol. 99 (American Geophysical Union, Washington, DC, 1997), pp. 9–16. <https://doi.org/10.1029/GM099p0009>
- R.A. Gummow, P. Eng, GIC effects on pipeline corrosion and corrosion control systems. *J. Atmos. Sol. Terr. Phys.* **64**(16), 1755–1764 (2002). [https://doi.org/10.1016/S1364-6826\(02\)00125-6](https://doi.org/10.1016/S1364-6826(02)00125-6)
- T. Iyemori, Storm-time magnetospheric currents inferred from mid-latitude geomagnetic field variations. *J. Geomagn. Geoelectr.* **42**(11), 1249–1265 (1990). <https://doi.org/10.5636/jgg.42.1249>

22. S. Jonas, E. McCarron, Recent U.S. policy developments addressing the effects of geomagnetically induced currents. *Space Weather* **13** (2015). <https://doi.org/10.1002/2015SW001310>
23. J. Kappenman, *Geomagnetic Storms and Their Impacts on the US Power Grid, Tech. Rep. Metatech Corp.* (Goleta, California, 2010)
24. J.G. Kappenman, in *Space Weather, Geophysical Monograph Series*, ed. by P. Song, H.J. Singer, G.L. Siscoe. Advanced Geomagnetic Storm Forecasting for the Electric Power Industry, Vol. 125 (American Geophysical Union, Washington, D.C., 2001), pp. 353–357. <https://doi.org/10.1029/GM125p0353> (2001)
25. J.G. Kappenman, Storm sudden commencement events and the associated geomagnetically induced current risks to ground-based systems at low-latitude and midlatitude locations. *Space Weather* **1**(3) (2003). <https://doi.org/10.1029/2003SW000009>
26. J.G. Kappenman, An overview of the impulsive geomagnetic field disturbances and power grid impacts associated with the violent Sun-Earth connection events of 29–31 October 2003 and a comparative evaluation with other contemporary storms. *Space Weather* **3**(8), 1–21 (2005). <https://doi.org/10.1029/2004SW000128>
27. G.V. Khazanov, *Space Weather Fundamentals* (CRC Press, Boca Raton, FL, 2016)
28. G.S. Lakhina, B.T. Tsurutani, Geomagnetic storms: historical perspective to modern view. *Geosci. Lett.* **3**(5), 1–11 (2016). <https://doi.org/10.1186/s40562-016-0037-4>
29. L.J. Lanzerotti, In *Space Weather, Geophysical Monograph Series*, ed. by P. Song, H.J. Singer, G.L. Siscoe. Space Weather Effects on Technologies, Vol. 125 (American Geophysical Union, Washington, D.C., 2001), pp. 1122. <https://doi.org/10.1029/GM125p0011> (2001)
30. M. Lehtinen, R. Pirjola, Currents produced in earthed conductor networks by geomagnetically-induced electric fields. *Ann. Geophys.* **3**(4), 479–484 (1985)
31. X. Li, M. Temerin, B.T. Tsurutani, S. Alex, Modeling of 1–2 September 1859 super magnetic storm. *Adv. Space Res.* **38**, 273–279 (2006). <https://doi.org/10.1016/j.asr.2005.06.070>
32. R.E. Lopez, D.N. Baker, J. Allen, Sun unleashes Halloween storm. *Eos Trans. AGU* **85**(11), 105–108 (2004). <https://doi.org/10.1029/2004EO110002>
33. N. Lugaz, C.J. Farrugia, C.W. Smith, K. Paulson, Shocks inside CMEs: a survey of properties from 1997 to 2006. *J. Geophys. Res. Space Phys.* **120**(4), 2409–2427 (2015). <https://doi.org/10.1002/2014JA020848>
34. N. Lugaz, C.J. Farrugia, C.-L. Huang, H.E. Spence, Extreme geomagnetic disturbances due to shocks within CMEs. *Geophys. Res. Lett.* **42**(12), 4694–4701 (2015). <https://doi.org/10.1002/2015GL064530>
35. N. Lugaz, C.J. Farrugia, R.M. Winslow, N. Al-Haddad, E.K.J. Kilpua, P. Riley, Factors affecting the geo-effectiveness of shocks and sheaths at 1 AU. *J. Geophys. Res. Space Phys.* **120**(11), 10,861–10,879 (2016). <https://doi.org/10.1002/2016JA023100>
36. T.S. Molinski, Why utilities respect geomagnetically induced currents. *J. Atmos. Sol. Terr. Phys.* **64**(16), 1765–1778 (2002). [https://doi.org/10.1016/S1364-6826\(02\)00126-8](https://doi.org/10.1016/S1364-6826(02)00126-8)
37. T.S. Molinski, W.E. Feero, B.L. Damsky, Shielding grids from solar storms. *IEEE Spectr.* **37**(11), 55–60 (2000). <https://doi.org/10.1109/6.880955>
38. C.M. Ngwira, A. Pulkkinen, L.-A. McKinnell, P.J. Cilliers, Improved modeling of geomagnetically induced currents in the South African power network. *Space Weather* **6**(11) (2008). <https://doi.org/10.1029/2008SW000408>
39. C.M. Ngwira, L.-A. McKinnell, P.J. Cilliers, A.J. Coster, Ionospheric observations during the geomagnetic storm events on 24–27 July 2004: long-duration positive storm effects. *J. Geophys. Res.* **117**(A9) (2012). <https://doi.org/10.1029/2011JA016990>
40. C.M. Ngwira, A. Pulkkinen, F.D. Wilder, G. Crowley, Extended study of extreme geoelectric field event scenarios for geomagnetically induced current applications. *Space Weather* **11**(3), 121–131 (2013). <https://doi.org/10.1002/swe.20021>
41. C.M. Ngwira, A. Pulkkinen, M.M. Kuznetsova, A. Glocher, Modeling extreme “Carrington-type” space weather events using three-dimensional global MHD simulations. *J. Geophys. Res. Space Phys.* (2014). <https://doi.org/10.1002/2013JA019661>
42. C.M. Ngwira, A.A. Pulkkinen, E. Bernabeu, J. Eichner, A. Viljanen, G. Crowley, Characteristics of extreme geoelectric fields and their possible causes: localized peak enhancements. *Geophys. Res. Lett.* **42**(17), 6916–6921 (2015). <https://doi.org/10.1002/2015GL065061>
43. D. Oliveira, Ionosphere-magnetosphere coupling and field-aligned currents. *Revista Brasileira de Ensino de Física* **36**(1), 1305 (2014). <https://doi.org/10.1590/S1806-11172014000100005>
44. D.M. Oliveira, Magnetohydrodynamic shocks in the interplanetary space: a theoretical review. *Braz. J. Phys.* **47**(1), 81–95 (2017). <https://doi.org/10.1007/s13538-016-0472-x>
45. D.M. Oliveira, J. Raeder, Impact angle control of interplanetary shock geoeffectiveness. *J. Geophys. Res. Space Phys.* **119**(10), 8188–8201 (2014). <https://doi.org/10.1002/2014JA020275>
46. D.M. Oliveira, J. Raeder, Impact angle control of interplanetary shock geoeffectiveness: a statistical study. *J. Geophys. Res. Space Phys.* **120**(6), 4313–4323 (2015). <https://doi.org/10.1002/2015JA021147>
47. D.M. Oliveira, J. Raeder, B.T. Tsurutani, J.W. Gjerloev, Effects of interplanetary shock inclinations on nightside auroral power intensity. *Braz. J. Phys.* **46**(1), 97–104 (2016). <https://doi.org/10.1007/s13538-015-0389-9>
48. D.M. Oliveira, E. Zesta, P.W. Schuck, H.K. Connor, E.K. Sutton, in *Proceedings of the 15th International Ionospheric Effects Symposium*, ed. by K.M. Groves, M.S. Magoun. Ionosphere-thermosphere global time response to geomagnetic storms, (Alexandria, VA, 2017)
49. R. Pirjola, Electromagnetic induction in the Earth by a plane wave or by fields of line currents harmonic in time and space. *Geophysica* **18**(1–2), 1–161 (1982)
50. R. Pirjola, Geomagnetically induced currents during magnetic storms. *IEEE Trans. Plasma Sci.* **28**(6), 1867–1873 (2000). <https://doi.org/10.1109/27.902215>
51. R. Pirjola, Review on the calculation of surface electric and magnetic fields and of geomagnetically induced currents in ground-based technological systems. *Surv. Geophys.* **23**(1), 71–90 (2002). <https://doi.org/10.1023/A:1014816009303>
52. P.R. Price, Geomagnetically induced current effects on transformers. *IEEE Power Engineering Review* **22**(6), 62–62 (2002). <https://doi.org/10.1109/MPER.2002.4312311>
53. A. Pulkkinen, S. Lindahl, A. Viljanen, R. Pirjola, Geomagnetic storm of 29–31 October 2003: geomagnetically induced currents and their relation to problems in the Swedish high-voltage power transmission system. *Space Weather* **3**(8) (2005). <https://doi.org/10.1029/2004SW000123>
54. A. Pulkkinen, E. Bernabeu, J. Eichner, C. Beggan, A.W.P. Thomson, Generation of 100-year geomagnetically induced current scenarios. *Space Weather* **10**(4) (2012). <https://doi.org/10.1029/2011SW000750>
55. P. Riley, J.J. Love, Extreme geomagnetic storms: probabilistic forecasts and their uncertainties. *Space Weather* (2017). <https://doi.org/10.1002/2016SW001470>
56. C. Russell, The solar wind interaction with the Earth’s magnetosphere: a tutorial. *IEEE Trans. Plasma Sci.* **28**(6), 1818–1830 (2000). <https://doi.org/10.1109/27.902211>
57. C.T. Russell, in *Space Weather, Geophysical Monograph Series*, ed. by P. Song, H.J. Singer, G.L. Siscoe. Solar wind and

- interplanetary magnetic field: a tutorial (American Geophysical Union, Washington, D.C, 2001), p. 125. <https://doi.org/10.1029/GM125p0073>
58. C.J. Schrijver, R. Dobbins, W. Murtagh, S.M. Petrinec, Assessing the impact of space weather on the electric power grid based on insurance claims for industrial electrical equipment. *Space Weather* (2014). <https://doi.org/10.1002/2014SW001066>
 59. C. Shen, Y. Chi, Y. Wang, M. Xu, S. Wang, Statistical comparison of the ICME's geoeffectiveness of different types and different solar phases from 1995 to 2014. *J. Geophys. Res. Space Phys.* **122** (2017). <https://doi.org/10.1002/2016JA023768>
 60. Y. Shi, E. Zesta, H.K. Connor, Y.-J. Su, E.K. Sutton, C.Y. Huang, D.M. Ober, C. Christodoulo, S. Delay, D.M. Oliveira, High-latitude thermosphere neutral density response to solar wind dynamic pressure enhancement. *J. Geophys. Res. Space Phys.* submitted (2017)
 61. V.M. Souza, D. Koga, W.D. Gonzalez, F.R. Cardoso, Observational aspects of magnetic reconnection at the Earth's magnetosphere. *Braz. J. Phys.* **47**(4), 447–459 (2017). <https://doi.org/10.1007/s13538-017-0514-z>
 62. B. Tsurutani, W.D. Gonzalez, G.S. Lakhina, S. Alex, The extreme magnetic storm of 1–2 September 1859. *J. Geophys. Res.* **108**(A7) (2003). <https://doi.org/10.1029/2002JA009504>
 63. B.T. Tsurutani, G.S. Lakhina, An extreme coronal mass ejection and consequences for the magnetosphere and Earth. *Geophys. Res. Lett.* **41**, 287–292 (2014). <https://doi.org/10.1002/2013GL058825>
 64. B.T. Tsurutani, D.L. Judge, F.L. Guarnieri, P. Gangopadhyay, A.R. Jones, J. Nuttall, G.A. Zambon, L. Didkovsky, A.J. Mannucci, B. Iijima, R.R. Meier, T.J. Immel, T.N. Woods, S. Prasad, L. Floyd, J. Huba, S.C. Solomon, P. Straus, R. Viereck, The October 28, 2003 extreme EUV solar flare and resultant extreme ionospheric effects: comparison to other Halloween events and the Bastille Day event. *Geophys. Res. Lett.* **32**(3) (2005). <https://doi.org/10.1029/2004GL021475>
 65. A. Viljanen, R. Pitjola, Geomagnetically induced currents in the Finnish high-voltage power system. *Surv. Geophys.* **15**(4), 383–408 (1994). <https://doi.org/10.1007/BF00665999>
 66. A. Viljanen, A. Pulkkinen, R. Pirjola, K. Pajunpää, P. Posio, A. Koistinen, Recordings of geomagnetically induced currents and a nowcasting service of the Finnish natural gas pipeline system. *Space Weather* **4**(10) (2006). <https://doi.org/10.1029/2006SW000234>
 67. C. Wang, J.B. Liu, H. Li, Z.H. Huang, J.D. Richardson, J.R. Kan, Geospace magnetic field responses to interplanetary shocks. *J. Geophys. Res.* **114**(A5) (2009). <https://doi.org/10.1029/2008JA013794>
 68. J.J. Zhang, C. Wang, T.R. Sun, C.M. Liu, K.R. Wang, GIC Due to storm sudden commencement in low-latitude high-voltage power network in China: observation and simulation. *Space Weather* **13**(10), 643–655 (2015). <https://doi.org/10.1002/2015SW001263>
 69. J.J. Zhang, C. Wang, T.R. Sun, Y.D. Liu, Risk assessment of the extreme interplanetary shock of 23 July 2012 on low-latitude power networks. *Space Weather* **14**(3), 259–270 (2016). <https://doi.org/10.1002/2015SW001347>